

## Evaluating Structural Capacity Reductions Due to Reinforcement Corrosion in Coastal Concrete Elements

S.M.D. Aguiar<sup>1</sup> and M.J. McCarthy<sup>2</sup>

<sup>1</sup>*School of Engineering & Built Environment, Edinburgh Napier University, Edinburgh, EH10 5DT, Scotland, e-mail: s.aguiar@napier.ac.uk*

<sup>2</sup>*Division of Civil Engineering, University of Dundee, Dundee, DD1 4HN, Scotland, UK, e-mail: m.j.mccarthy@dundee.ac.uk*

### ABSTRACT

Global sea levels are rising due to climate change and reinforced concrete coastal structures are essential components of defence against associated effects including, flooding and coastline erosion. The high chloride content of these environments is a major cause of reinforcement corrosion and consequently potential structural capacity reduction. In this paper, real-size reinforced concrete walls under both sustained loading and continuous exposure to chloride-laden conditions were investigated. The experimental programme was carried out mainly by destructive tests made periodically over 24 months. These enabled the effects of loading and subsequent flexural cracking (intersecting cracks) on corrosion propagation, and structural capacity and stiffness to be quantified. The results showed that corrosion was greater when flexural cracks were present and that reductions in structural capacity and stiffness increased as the process developed. Design calculations based on reinforcement losses and concrete strength reductions during exposure tended to over-estimate damage occurring.

**Keywords.** Reinforced concrete, Coastal structures, reinforcement corrosion, structural capacity and stiffness reduction.

### INTRODUCTION

Research on reinforcement corrosion in concrete has been on-going for more than 30 years and has covered many aspects of this damaging process. These have included (i) investigations of the causes and mechanisms involved, (ii) development of electrochemical techniques for monitoring and controlling deterioration (laboratory and field), and (iii) employment of protection methods preventing initiation and propagation, (as noted by Rincón et al (2007)). As a result, a good understanding of material behaviour has been developed and techniques for extending service-life exploited.

One area where less attention has been given is the effect of the process on the structural capacity of reinforced concrete members (as reviewed and noted by Aguiar, 2008). Indeed, much of the research carried out in this area has tended to focus on small-scale samples. Furthermore, effects such as cracks occurring in concrete and loading of structural members during service with regard to chloride exposure have only received coverage in a few studies, but are likely to influence the degree of damage occurring. These aspects of the

deterioration process assume increasing importance given that (i) greater attention is being given to whole-life cycle analysis of structures and (ii) with climate change, concrete is more frequently being exposed to extreme weather conditions.

The work reported in this paper describes research concerned with concrete exposed to simulated coastal conditions and to quantifying the effects indicated above on the chloride-induced corrosion process and associated damage.

## EXPERIMENTAL PROGRAMME

The test programme comprised: (1) quantitative control of environmental parameters (i.e. wetting and drying cycles, temperature and humidity) to promote the deterioration process; (2) use of test elements of structurally significant size, (3) simultaneous application of service loads (allowing the effects of cracking of the concrete surface to be considered) and saltwater spray and (4) evaluation of damage using structural tests and losses in steel and concrete properties during exposure.

### Materials and Mix Proportions.

A Portland cement of strength class 42.5 N to BS EN 197-1: 2011 was used. The aggregates comprised natural gravel of maximum size 20 mm, with medium grade sand to BS EN 12620: 2002 + A1: 2008. The concrete used was of low strength class (C25/30), compared to that likely to be used in chloride exposures, to enable rapid chloride transportation with respect to the test timescale available. Details of the mix proportions for the concrete, which had a nominal slump of 75 mm, are given in Table 1.

**Table 1. Concrete mix proportions (kg/m<sup>3</sup>)**

PC 42.5	20mm gravel	10mm gravel	Sand	water
270	720	395	800	180

### Structural Elements and Test Probes

The large-scale reinforced concrete (large cantilever walls) used, were designed in accordance with Eurocode 2 (BS EN 1992-1-1: 2005) and BS 6349-1, 2000. These calculations were made by following the simplified rectangular stress block, (Eurocode 2). Their dimensions for width, height and thickness were 1000 x 2000 x 150 mm, respectively and they were supported on concrete footings cast at the same time, see Figure 1. The elements contained transverse and longitudinal reinforcement (load factors not taken into account) of 10 mm diameter (high yield bars), located at a cover depth of 30 mm. Details of the reinforcement used are shown in Table 2. The section of the element was considered to be under-reinforced and it was expected that steel would yield before crushing of concrete occurred. This was also adopted to ensure corrosion-induced damage would have a greater influence on structural capacity and damage would occur in a reasonable time scale.

Steel probes (working electrodes) were cast at selected positions: 3 probes at the base (high tensile zone) and 1 each at the middle and top of the element (150 mm from the top edge) to monitor reinforcement corrosion, see Figure 2. The top and middle areas allowed investigation of corrosion in uncracked concrete. The probes at the bottom were placed to investigate corrosion in cracked concrete.

**Table 2. Main and secondary steel in the large-scale elements**

Cover (mm)	Main steel (over wall width)			Secondary steel (per metre)		
	$A_s$ ( $mm^2$ )	$\rho$ (%)	Reinforc.	$A_s$ , min. ( $mm^2$ )	$\rho$ (%)	Reinforc./meter
30	471	0.41	6T10	195	0.17	4T10

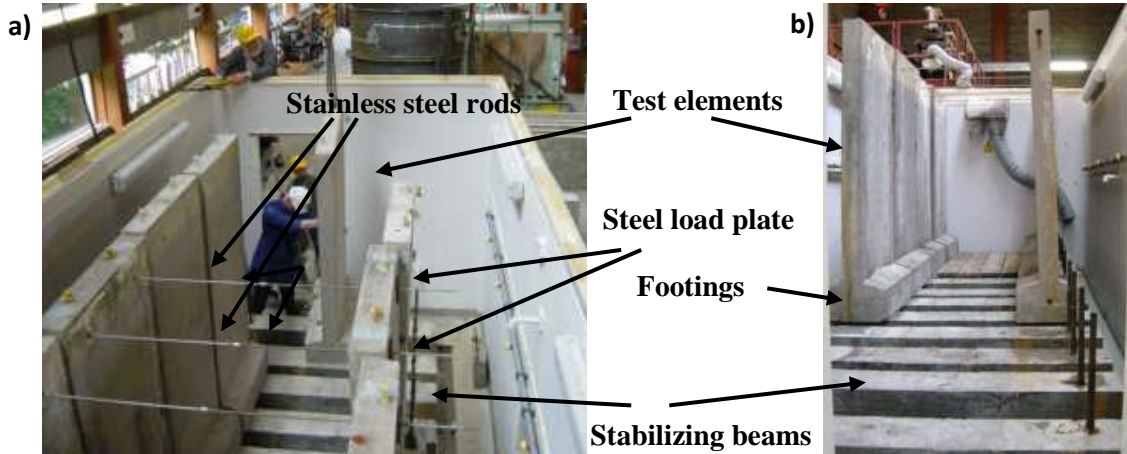


**Figure 1. Test elements a) being placed in the environmental chamber and loaded and b) on the supporting beams.**

### Application of Sustained Loading

The test elements were placed in the environmental chamber in pairs and were loaded by two cables (stainless steel rods) placed at the top of each wall (150 mm from the upper), as illustrated in Figure 1. In addition, large beams were used to stabilize each pair of walls to avoid any movement while they were being loaded and during exposure (see also Figure 1). The load applied at the top of the cantilever was 70% of the ultimate design strength (capacity) of the elements, in order to represent the hydraulic pressure under service conditions found in sea-walls. A flat steel plate and a load cell were used at each end of the stainless steel rods to apply the loading to the elements, which was kept constant during the testing period (24 months).

Transverse cracks were formed at the base of each wall as a result of the load application at the top of the cantilever (region of the cantilever wall just above the concrete footing). The load was checked periodically and if any variation was observed, then a re-load procedure was carried out. The cracks at the base of the walls intersected the 3 steel probes placed in this region.

### Non-destructive and Destructive Load Tests

The corrosion activity of the probes was evaluated by two non-destructive tests: half-cell potential and linear polarization using a silver/silver chloride (Ag/AgCl) reference electrode, following the method of Dhir et al (1994). These tests were carried out throughout the full 8,

16 and 24 months exposure. The effect of corrosion on the structural capacity (ultimate flexural bending capacity) and stiffness (ultimate deflection) was quantified by carrying out destructive tests (load and rebar diameter reduction).

These were carried out on the elements until failure at exposure periods of 0 (control), 8, 16 and 24 months. For this purpose, an auxiliary frame to give similar loading conditions to those in the environmental chamber during exposure was designed and used, see Figure 3. The calculated (design) ultimate strength of the concrete walls was used as a reference for the application of load to failure. As soon as the applied loading reached 90% of the ultimate calculated strength, the test was controlled by deflection using a plumb line with an increment of 20 mm for each load application until failure occurred. The plumb line was used as a reference line with controlled distances from the top and base of each cantilever wall.

After the destructive load test was completed, samples of the main longitudinal steel reinforcement were removed at the base (cracked condition and where the moment was maximum) of the walls and the remaining cross-section was measured with a digital Vernier caliper in order to directly determine the metal loss. In testing the main reinforcement, this ensured that macrocell effects were taken into account and that loss of steel could be directly related to changes in structural capacity. Tests were also made on concrete cores, removed from the elements, for compressive strength during exposure, to quantify any losses. These were then used to calculate the corresponding reduction in structural resistance (flexural capacity and stiffness) of the elements at the end of the exposure periods. These were carried out using the approach adopted in the original design.

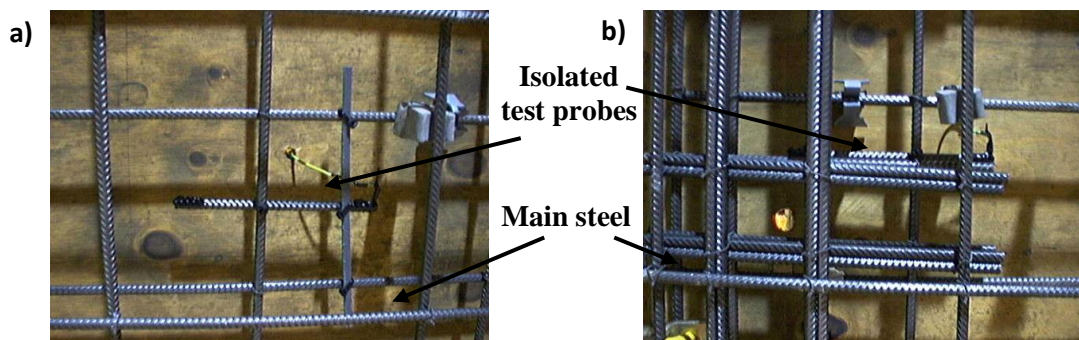


**Figure 2. Placement of probes a) in the middle and b) at the top of the walls (more congested area).**

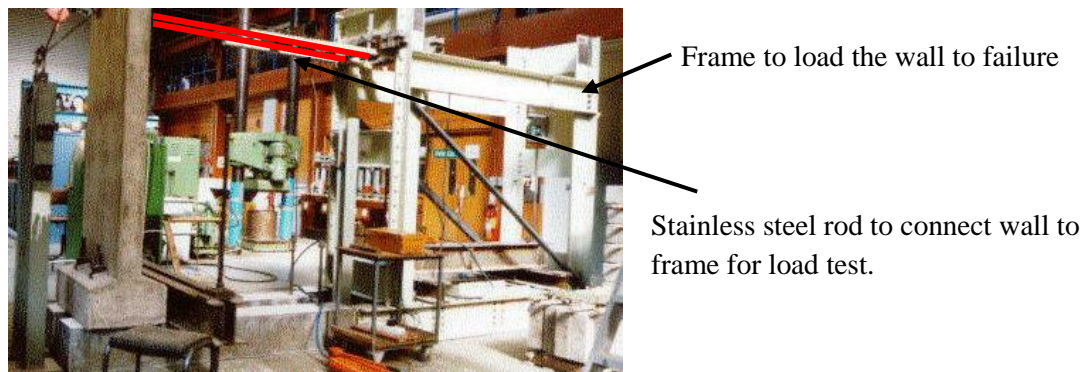


**Figure 3. Load test method including wall and auxiliary frame.**

## REINFORCEMENT CORROSION

Figure 4a) shows that corrosion potentials of the probes decreased rapidly during the first 2.5 months exposure in the environmental chamber. Thereafter, the values tended to level off between

-400 and -500 mV and remained approximately constant until 24 months. Despite more negative corrosion potentials in the cracked concrete, the results suggest corrosion was occurring regardless of whether or not the concrete was cracked. Corrosion currents of the probes also increased rapidly during the first month suggesting that corrosion initiated at this time, see Figure 4b). After this, the rate of change in corrosion current slowed down beyond 2 months. However, in contrast to the corrosion potentials, corrosion currents continued to increase slowly for the remaining exposure duration. During this period these were in the range of 5.0 to 47.7  $\mu\text{A}/\text{cm}^2$  (58.0 to 553.4  $\mu\text{m}/\text{year}$ ) in uncracked concrete and 6.0 to 76.8  $\mu\text{A}/\text{cm}^2$  (69.6 to 891.2  $\mu\text{m}/\text{year}$ ) in cracked concrete, suggesting that propagation was more severe in the latter.

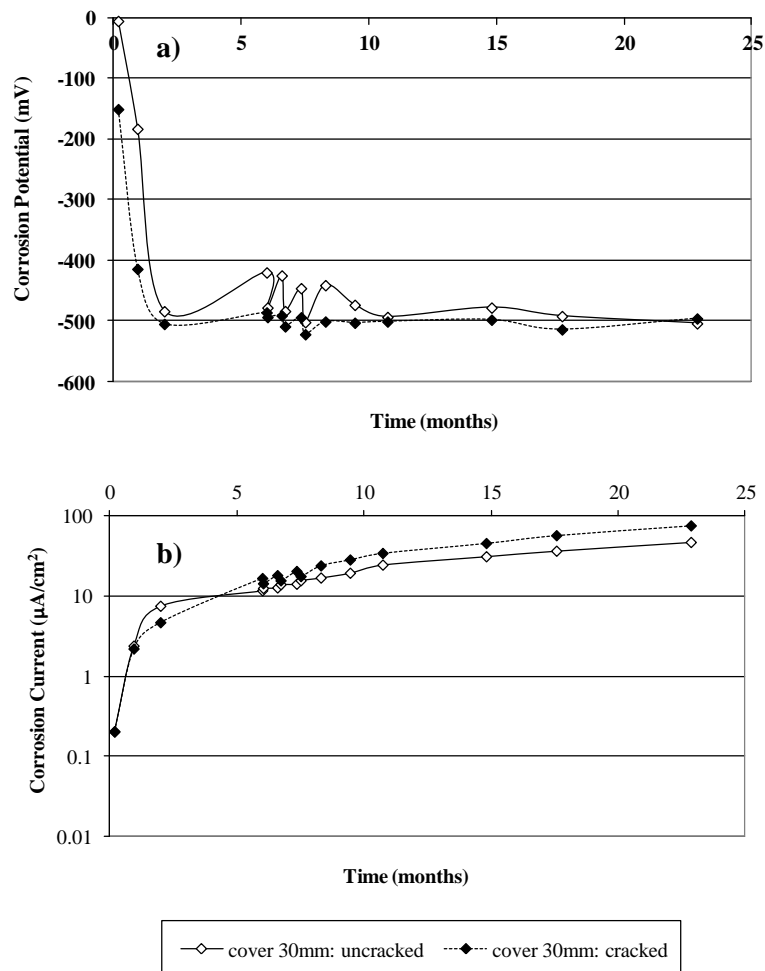


**Figure 4. Development of a) corrosion potential and b) corrosion current with time (uncracked and cracked areas).**

The influence of cracks on corrosion propagation can be considered and categorised in two ways: coincident and intersecting cracks. The former seem to break down the passivity of steel at many locations, and contribute to an acceleration of the rate of corrosion if oxygen and moisture are readily transmitted to cathodic areas through cracks (Committee 224.1R, 1993 and Concrete Society, 1995). With intersecting cracks, on the other hand, the influence of crack width on the rate of corrosion has been found to be negligible (Beeby, 1978; ACI Committee 224.1R, 1993; Concrete Society, 1995). Schiessl and Raupach (1997) and Francois and Arliguie (1999), based on their long-term experimental work, further concluded that intersecting crack widths in the range 0.1 to 0.5 mm do not influence the degree of chloride-induced corrosion. Furthermore, Schiessl and Raupach observed that corrosion propagation at the crack decreased with time and was independent of its width. Results presented by the CEB (1989) and Broomfield (1997) suggest that the influence of intersecting cracks up to about 0.4 to 0.5 mm is relatively small, and any on-going corrosion is likely to reduce to insignificant levels due to self-healing effects. Since corrosion propagation rates in intersecting cracked concrete are governed by similar factors to those of uncracked concrete (Beeby, 1978; ACI Committee 224.1R, 1993; Concrete Society, 1995; Schiessl and Raupach (1997) and Bentur et al, 1997), it is likely that the quality of the material (as influenced by mix design and curing) and the cover depth are more important in controlling the process and its rate at cracks, than their widths.

The findings observed in the current work are supported by Li, (2001) and Torres-Acosta et al, (2007), which suggest the existence of intersecting cracks may promote corrosion. In addition, a sustained load was applied and kept constant during the full testing period, which caused cracking in the tensile zone of the elements (base of cantilever walls). Furthermore, this is likely to prevent self-healing and thereby facilitate corrosion (Torres-Acosta et al, 2007). This situation is known to promote macrocell corrosion with the anode area being located in the steel at the crack and the large cathode area of reinforcing steel remote from this. As noted by Raupach (1996), generally the loss of steel at the anode occurs at a very high rate due to differences in cathode/anode areas. The metal loss of the reinforcing steel measured from the recovered steel at the cracked areas was about 6, 13 and 18% at 8, 16 and 24 months exposure. At the uncracked areas, adjacent to the intersecting cracks, no corrosion was observed on the same recovered steel, bars.

## **LOAD/DEFLECTION BEHAVIOUR**

Figure 5 indicates that both flexural capacity and deflection reduced with increasing corrosion propagation (exposure time). The control elements not only showed higher ultimate flexural strength but also gave greater ultimate deflection (i. e. deformed to a greater degree before failure).

As corrosion develops, the stiffness of the elements decreases, suggesting that ductility decreases with reduced structural resistance (reduction in flexural capacity and deflection). Abdullah et al (1996) and Almusallam et al (1996) reported similar findings when investigating RC slabs. Lee et al (1998) tested the effect of corrosion on simply-supported beams and found these gave ductile failures with long plateaus after peak load. It was also found that beyond a certain corrosion level, stiffness was lower and the peak noticeably reduced. In the current research, it was observed that the elements with 18% rebar reduction gave a significant drop in ductility and the peak load reduced by about 23% compared to that of the uncorroded element. The corresponding deflection measured for the corroded elements reduced by about 17%. Du et al (2005) investigated the effect of corrosion on the ductility of steel reinforcement with different surface conditions, diameters and steel classes.

They observed that the ductility of reinforcing steel considerably reduced as corrosion increased. This also appears to be reflected in the results obtained in the current study.

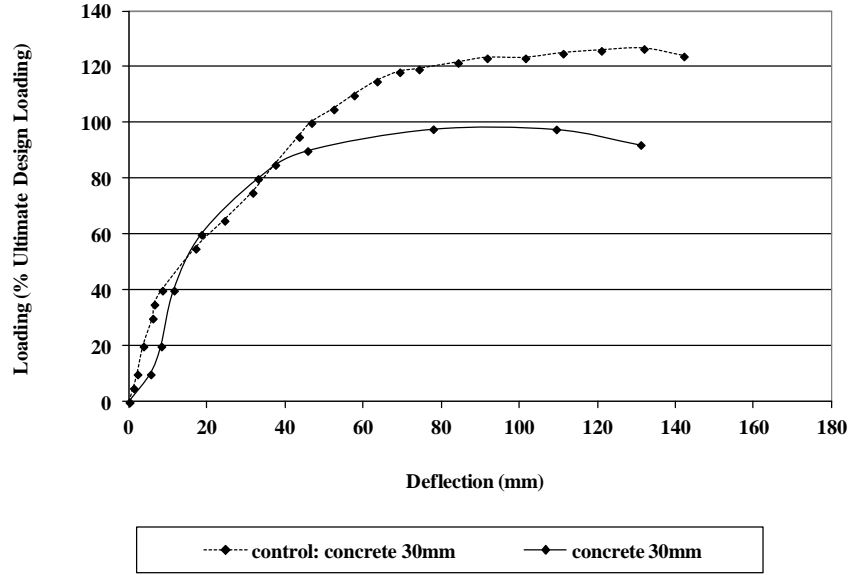


**Figure 5. Load/deflection curves from the destructive load tests at the end of the exposure period (24 months).**

#### **FLEXURAL CAPACITY / MATERIAL DETERIORATION COMPARISONS**

By considering the losses in cross-section noted in the previous section and the changes in concrete strength, it is possible to re-calculate the flexural capacity of the elements allowing for the deterioration in materials taking place. Tests for compressive strength showed that this decreased with increasing exposure period by about 4, 6 and 9% at 8, 16 and 24 months, respectively. Compressive strength reductions of low nominal strength PC concrete when exposed to a marine environment has also been observed in other studies. Thomas and Matthews (1991 and 2004) observed that the compressive strength of PC decreased by about 1.5 to 3% after 2 years exposure compared to that at 28 days (water-cured). After 10 years exposure, this had increased to about 30%.

The ultimate flexural bending capacity determined for the elements tested and by considering the materials was considered by adopting a deterioration factor proposed by Li (2003b; Li and Zheng 2005):

$$\varphi(t) = \frac{M(t)}{M_0} \quad (\text{Eq. 1})$$

where;  $\varphi(t)$  is the deterioration function factor for bending capacity,  $M(t)$  is the ultimate flexural bending capacity of the element at time  $t$ , and  $M_0$  is the initial bending capacity. The advantage of this equation is the use of relative, rather than absolute, values for quantifying deterioration:

$$\varphi(t) \leq 100\% \quad (\text{Eq. 2})$$

This relative measure enables the normalisation of test results for test elements with different concrete strength and cross-sections, thereby maximising the use of the test results.

From Table 4 it can be seen that the ultimate flexural capacity of the uncorroded elements was about 50% higher than that from the calculations (design ultimate flexural capacity). Figure 6 shows that the reduction in calculated ultimate flexural capacity increased sharply with exposure time. The destructive load test, however, shows a less significant reduction in ultimate flexural capacity. As a result, the difference tends to increase with time, suggesting that material deterioration tests overestimate the reduction in flexural capacity. This difference suggests that stress redistribution occurring during the load test may increase the structural resistance of the elements, resulting in a greater ultimate flexural capacity. Furthermore, a small cover depth (30 mm) and a low strength class concrete were used in the study, which may have contributed to a porous near-surface and provided both better accommodation of the expansive corrosion products by concrete and additional interlocking effects. These may have improved the bond between the reinforcing steel and surrounding concrete, thereby enhancing the structural resistance of the elements.

**Table 4. Ultimate flexural capacity (calculated and measured of the control elements,  $\mu_u = P_u \times 1.85$  (lever arm)) and deflection (calculated and measured)**

Ultimate design (calculated)		Ultimate resistance of uncorroded elements (load test) (**)	
Flexural capacity (*) (kN.m)	Deflection (mm)	Flexural capacity (kN.m)	Deflection (mm)
23.8	66.4	35.2	131.8

(\*) safety factors were not used in these calculations,

(\*\*) these elements were tested after being exposed for 1 year to the laboratory environment.

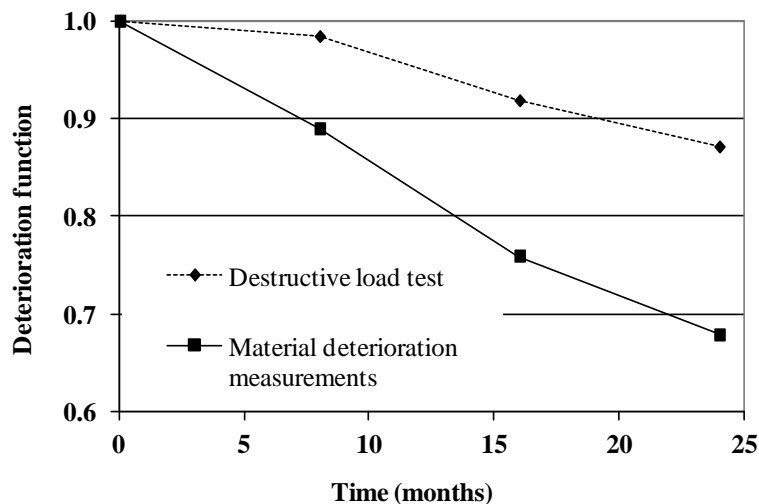


**Figure 6. Comparison of flexural capacity reduction in the elements determined by different tests.**

The flexural capacity was also determined by using a simplified rectangular stress block (Eurocode 2). The adoption of this approach and the changes in section resulting from the



damage occurring to the materials may also have an influence on the comparisons made. This represents an area being further examined by the Authors.

## CONCLUDING REMARKS

The results from both corrosion potential and corrosion current tests showed that this appeared to initiate very rapidly in the first 2.5 to 3 months of exposure to the chloride-laden environment. Additionally, corrosion current measurements indicated that propagation was more severe when flexural cracking was present (greater than 0.1 mm), at the exposure test times: 8, 16 and 24 months. It is also likely that macrocell corrosion was occurring in the main reinforcement where the embedded steel at the cracks acted as small anodic areas, while the remaining steel acted as large cathodic areas, supporting significant local metal loss.

In general, the reduction in both structural capacity and deflection (stiffness) increased as corrosion propagated. The work also indicated that both low strength class concrete and existing flexural cracks appeared to accommodate the expansive corrosion products which possibly improved the interlocking effects between the embedded steel rebars and surrounding concrete. This may have given a better bond at the steel/concrete interface, therefore, affecting the reduction in structural resistance (flexural capacity and deflection) during the load test.

The material deterioration (steel and concrete) occurring was also evaluated and used to calculate (using Eurocode 2) the reduction in structural capacity. This gave greater losses than those determined in the load tests.

## ACKNOWLEDGEMENTS

The current authors acknowledge the support of the Engineering and Physical Sciences Research Council (EPSRC), UK, under grant GR/R28348/01. The contribution from Professor Chun Q. Li is gratefully acknowledged.

## REFERENCES

- Abdullah A. A., Al-Gahtani, A. S., Abdur Rauf Aziz, and Rasheeduzzarar, (1996). "Effect of Reinforcement Corrosion on Flexural Behavior of Concrete Slabs". *Journal of Materials in Civil Engineering, ASCE*, Vol.8, No.3, Aug., 123-127.
- ACI Committee 224.1R – 93, (1993). *Causes, Evaluation and Repair of Cracks in Concrete Structures*. ACI, Detroit, USA.
- Almusallam, A. A., Al-Gahtani, A. S., Aziz, A. R., Dakhil, F. H. and Rasheeduzzafar, (1996). "Effect of Reinforcement Corrosion on Flexural Behaviour of Concrete Slabs". *ASCE, Journal of Materials in Civil Engineering*, Vol.9, No.3, Aug., 123-127.
- Ballim, Y., Reid, J. C. and Kemp, A.R., (2001). "Deflection of RC Beams under Simultaneous Load and Steel Corrosion". *Magazine of Concrete Research*, Vol.53, No.3, 171-181.
- Aguiar, S.M.D., (2008). *An Investigation of Corrosion-Induced Structural Deterioration in RC Coastal elements*. Internal report, Division of Civil Engineering, University of Dundee, Scotland.
- Beeby, A. W. (1978). "Corrosion of Reinforcing Steel in Concrete and Its Relation to Cracking". *The Structural Engineer*, Vol. 56A, No.3, Mar, 77-81.

- 
- Bentur, A., Diamond, S. and Berke, N. S., (1997). *Modern Concrete Technology 6: Steel Corrosion in Concrete, Fundamentals and Civil Engineering Practice*, E & FN Spon, London.
- Broomfield, J. P., (1997). *Corrosion of Steel in Concrete, Understanding, Investigation and Repair*, E & FN Spon, London.
- BS 6349-1: 2000: *Marine Structures – Code of Practice of General criteria*, BSI, London.
- BS EN 12620: 2002+A1: 2000: *Aggregates for Concrete*, BSI, London.
- BS EN 1992-1-1: 2005: *EUROCODE 2. Design of Concrete Structures. General Rules and Rules for Building*, BSI, London.
- BS EN 197-1: 2000: *Cement – Part 1. Composition, Specification and Conformity Criteria for Common Cements*, BSI, London.
- Cabrera, J. G., and Ghoddousi, P., (1992). “The Effect of Reinforcement Corrosion on the Strength of the Steel/Concrete Bond. In: *Proceedings of the Conference on Bond in Concrete*, Latvia, CEB, 11-24.
- CEB (1989). *Durable Concrete Structures – Design Guide*, 2<sup>nd</sup> Edition. T. Telford, London.
- Concrete Society, (1995). “The Relevance of Cracking in Concrete to Corrosion of Reinforcement”. Technical Report N° 44, *The Concrete Society*, Slough, UK.
- Dhir, R.K., Jones, M.R. and McCarthy, M.J., (1994). “PFA Concrete: Chloride-Induced Reinforcement Corrosion. *Mag. Conc. Res.*, Vol.46, No.109, 269-278.
- Du, Y.G., Clark, L.A. and Chan, A.H.C., (2005). “Effect of Corrosion on Ductility of Reinforcing Bars”. *Mag. Conc. Res.*, Vol.57, No.7, Sept., 407-419.
- Francois, R. and Arliguie, G., (1999). “Effect of Microcracking and Cracking on the Development of Corrosion in Reinforcement Concrete Members”. *Mag. Conc. Res.*, Vol.51, No.2, Apr., 143-150.
- Lee, H. S., Noguchi, T. and Tomosawa, F., (1998). “FEM Analysis for Structural Performance of Deteriorated RC Structures due to Rebar Corrosion”. *Concrete under Severe Conditions: Environment and Loading*, CONSEC’98, E & F N Spon, 327- 336.
- Li, C. Q., (2001). “Initiation of Chloride-Induced Reinforcement Corrosion in Concrete Structure Members – Experimentation”. *ACI Structural Journal*, Vol.98, No.4, Jul-Aug, 502-510.
- Li, C. Q., (2003). “Life cycle Modelling of Corrosion Affected Concrete Structures – Propagation”. *Journal Structural. Engineering.*, A.S.C.E., Vol.129, No.6, 753-761.
- Li, C. Q., and Zheng, J. J., (2005). “Propagation of Reinforcement Corrosion in Concrete and its Effects on Structural Deterioration”. *Mag. Conc. Res.*, Vol.57, No.5, June, 261-271.
- Raupach, M. (1996). “Chloride-Induced Macrocell Corrosion of Steel in Concrete – Theoretical Background and Practical Consequences”. *Construction and Building Materials*, Vol.10, No.5, 329- 338.
- Rincón, O.T. and et al (2007). “Effect of the Marine Environment of RC Durability in Iberoamerican Countries: DURACON Project/CYTED”. *Corrosion Science*, Vol.49, 2832-2843.
- Schiessl, P. and Raupach, M., (1997). “Laboratory Studies and Calculations on the Influence of Crack Width on Chloride-Induced Corrosion of Steel in Concrete”. *ACI Materials Journal*, Vol.94, No.1, Jan – Feb, 56-62.
- Thomas, M. D. A.. and Matthews, J. D., (1991). *Durability studies of PFA concrete*. BRE Information paper, N.30, HMSO.
- Thomas, M. D. A.. and Matthews, J. D., (2004). “Performance of pfa in a Marine Environment – 10 Years Results”, *Cem. & Conc. Composites*, 26, 5-20.
- Torres-Acosta, A. A. and Martínez-Madrid, (2007). “Residual Flexure Capacity of Corroded Reinforced Concrete Beams”. *Engineering Structures*, Vol.29, 1145-1152.